AIAA 81-0052R

Prediction and Experimental Verification of Transient Airfoil Motion

Stephen M. Rock*
Systems Control Technology, Palo Alto, Calif.
and
Daniel B. DeBra†
Stanford University, Stanford, Calif.

The theory for aerodynamic loading associated with transient motion of an airfoil in a wind tunnel has been extended and verified experimentally. A generalized Theodorsen function which includes wall effects is described and finite-state approximations are developed for large wing-semichord/wall-spacing ratios. Finally, experimental results are presented which verify the theoretical predictions for transient airfoil motions. These results were obtained using a small, low-subsonic wind tunnel with a unique airfoil suspension design that provides uncoupled sensing and actuation for two degrees of freedom.

Introduction

A TREND in modern aircraft design is toward sophisticated active control systems to influence the aeroelastic behavior. The goal is to increase service life, decrease structural weight (and hence fuel consumption), and increase performance. These goals are feasible. Examples of successful demonstrations in actual flights are the B-52 load alleviation and mode stabilization (LAMS) program,[1] the B-52 CCV program,[2] and the C-5A active load distribution control system.[3]

Effective implementation of these control systems depends heavily upon the accuracy of the aerodynamic theory in predicting the loads associated with general motions of the lifting surfaces. However, this theory has been only partially verified. Experimental studies which have been performed concentrated on airfoils that were either stationary or oscillating sinusoidally.[4-10] To the authors' knowledge, no experimental program was directed at verifying the aerodynamic loading associated with more general airfoil motion.

Extending aerodynamic theory to predict loadings associated with general motions of an airfoil has not been trivial. Theodorsen first wrote the equations for an oscillating airfoil in 1935.[11] Technically, however, his derivation required diverging oscillations of the airfoil to insure convergence of integrals appearing in his "Theodorsen function." His results were extended to include simple harmonic motion due largely to the availability of experimental data which supported the predictions of the theory. It was not until 1977 when Edwards[12] identified a derivation of the generalized Theodorsen function in the work of von Kármán and Sears[13,14] that the validity of the theory for general motions was accepted.

In addition to extending the theory, this paper describes the experimental verification of the aerodynamic lift and moment expressions for transient motions of an airfoil. The object of experimental verification is the flutter locus for the ideal two-degree-of-freedom (DOF) typical section in a small wind tunnel with low-subsonic flow. This flutter locus is a plot of the system eigenvalues as functions of airspeed. Consequently, it is a basic description of the system dynamics.

Presented as Paper 81-0052 at the AIAA 19th Aerospace Sciences Meeting, St. Louis, Mo., Jan. 12-15, 1981; submitted March 12, 1981; revision received Aug. 31, 1981.

*Program Manager.

†Professor.

Equations of Motion (Freestream)

The system chosen for study in this work is the ideal two-DOF typical section. This is a concept which was introduced in the 1930s by Theodorsen and Garrick.[11,15] They suggested using a simple two-DOF model with properties characteristic of a typical section of a wing at 75% span to predict the aeroelastic properties of the wing as a whole. Their model is useful because it is simple enough to be understood easily, yet it is sufficiently complex to demonstrate such aeroelastic phenomena as divergence and bending-torsion flutter.

The ideal two-DOF typical section is shown in Fig. 1. It consists of an infinitely thin rigid airfoil that can plunge vertically against a linear spring k_h and pitch about its elastic axis against a torsional spring k_α. The airflow is assumed to be two-dimensional and incompressible. All quantities are given per unit span.

The equations describing pure oscillatory motion of this system are well known[11,15,16]

$$m(i\omega)^2 h + k_h h + s_\alpha (i\omega)^2 \alpha = -F - L \tag{1a}$$

$$I_\alpha (i\omega)^2 \alpha + k_\alpha \alpha + s_\alpha (i\omega)^2 h = M + T \tag{1b}$$

where $L(\omega)$, the Fourier transform of the aerodynamic lift, is given by

$$L(\omega) = \pi\rho b^2 [(i\omega)^2 h + U(i\omega)\alpha - ba(i\omega)^2 \alpha] + 2\pi\rho UbC(k)[(i\omega)h + U\alpha + b(\tfrac{1}{2} - a)(i\omega)\alpha] \tag{2a}$$

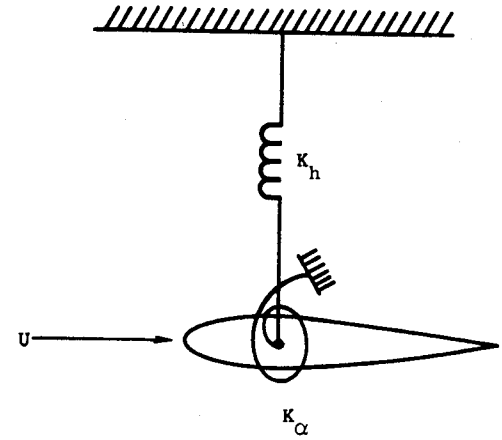

Fig. 1 Ideal two-degree-of-freedom typical section.

and M, the aerodynamic moment about the elastic axis, is given by

$$M(\omega) = \pi\rho b^2 [ba(i\omega)^2 h - b^2(\tfrac{1}{8} + a^2)(i\omega)^2\alpha - Ub(\tfrac{1}{2} - a)(i\omega)\alpha] + 2\pi\rho Ub^2(a + \tfrac{1}{2})C(k)[(i\omega)h + U\alpha + b(\tfrac{1}{2} - a)(i\omega)\alpha] \quad (2b)$$

The terms F and T represent any externally applied forces and torques at or about the elastic axis, and $C(k)$ is the Theodorsen function. The remaining terms appearing in Eqs. (1) and (2) are defined in Fig. 2 and Table 1. All quantities are expressed per unit span. k is the reduced frequency.

The sign convention for h, the plunge motion, is positive downward; α, the pitch motion, is positive "nose up." Care should be taken since the sign convention varies throughout the literature and since the coordinate system differs from the NACA body-fixed system for stability analysis.

Equations (1) and (2) may be rewritten in nondimensional form

$$(i\omega)^2\bar{h} + \omega_h^2\bar{h} + x_\alpha(i\omega)^2\alpha = -\bar{F} - \bar{L} \quad (3a)$$

$$(i\omega)^2\alpha + \omega_\alpha^2\alpha + \frac{x_\alpha}{r_\alpha^2}(i\omega)^2\bar{h} = \bar{T} + \bar{M} \quad (3b)$$

where $\bar{h} = h/b$ and

$$\bar{L} = \frac{1}{\mu}[(i\omega)^2\bar{h} + \bar{U}(i\omega)\alpha - a(i\omega)^2\alpha] + \frac{2}{\mu}\bar{U}C(k)[(i\omega)\bar{h} + U\alpha + (\tfrac{1}{2} - a)(i\omega)\alpha] \quad (4a)$$

$$\bar{M} = \frac{1}{\mu r_\alpha^2}[a(i\omega)^2\bar{h} - (\tfrac{1}{8} + a^2)(i\omega)^2\alpha - \bar{U}(\tfrac{1}{2} - a)(i\omega)\alpha] + \frac{2}{\mu r_\alpha^2}\bar{U}(a + \tfrac{1}{2})C(k)[(i\omega)\bar{h} + U\alpha + (\tfrac{1}{2} - a)(i\omega)\alpha] \quad (4b)$$

The parameters appearing in Eqs. (3) and (4) are defined in Table 2.

The equations outlined above are for freestream and an infinitely thin airfoil. If the airfoil has finite thickness and is placed in a flowfield bounded by tunnel walls, the aerodynamic lift and moment expressions must be modified. The modifications are of two basic types: blockage corrections and lift interference effects. Blockage corrections account for the reduction in available cross-sectional area when a body of finite thickness is placed in a bounded flowfield. These corrections may be divided into solid blockage terms and wake blockage terms, which refer to the finite thickness of an airfoil and its wake, respectively.

Blockage corrections amount to a correction on the airspeed. Specifically,

$$U = (1 + \epsilon_{wb} + \epsilon_{sb})U_{uc} \quad (5)$$

where U_{uc} is the uncorrected freestream flow velocity.

Convenient outlines of the procedure to calculate ϵ_{wb} and ϵ_{sb} are provided in Refs. 17 and 18. The corrections are assumed independent of each other and of the lift. The results for a NACA 0009 airfoil with an H/b ratio of 2, where the tunnel height is $2H$ and the wing chord is $2b$ (characteristic of the experimental apparatus used in this investigation), is a 1.2% increase in the airspeed. It is assumed that any frequency dependence is negligible.

Lift interference effects account for the alteration to the flowfield produced by the wind-tunnel walls. These effects result from the boundary condition that the wall be a streamline of the flow. These effects are frequency dependent.

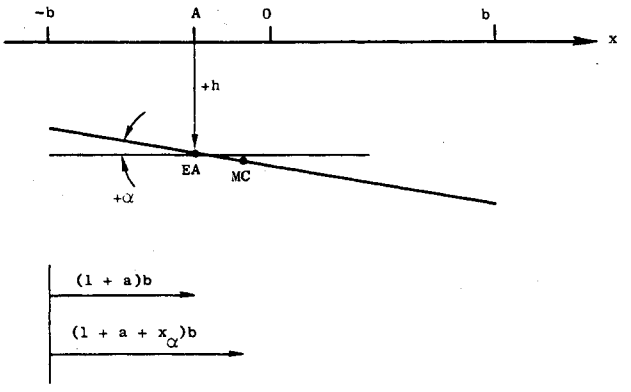

Fig. 2 Definition of parameters.

Table 1 Definition of parameters

Parameter	Definition	Units
a	Distance in semichords elastic axis lies aft of midchord	—
b	Semichord = $c/2$	m
m	Mass per unit span	kg/m
I_α	Moment of inertia about elastic axis per unit span	kg·m²/m
k_h	Plunge spring rate per unit span	(N/m)/m
k_α	Torsional spring rate per unit span	N·m/m
S_α	Inertia cross coupling per unit span	kg·m
U	Airspeed	m/s
ρ	Air density	kg/m³

Table 2 Definition of parameters

Parameter	Definition	Units
μ	Mass ratio: $m/\pi\rho b^2$	—
x_α	S_α/mb	—
r_α^2	Radius of gyration: I_α/mb^2	—
ω_h	Plunge natural frequency (in vacuo)	s^{-1}
ω_α	Pitch natural frequency (in vacuo)	s^{-1}
k	Reduced frequency: $\omega b/U$	—
$\bar{U}$	Normalized airspeed: U/b	s^{-1}
$\bar{h}$	Normalized displacement: h/b	—

Wind-Tunnel Wall Effects: Lift Interference

Lift interference effects due to wind-tunnel wall have been evaluated in two ways. The first is an approximate solution by Reissner,[19] the second an exact solution by Timman.[20] Both consider an infinitely thin airfoil spanning the width of a rectangular tunnel equidistant from and parallel to the top and bottom walls. Airflow is two-dimensional and incompressible, and the airfoil is assumed to move in simple harmonic motion with infinitely small amplitude.

Reissner's solution is approximate. However, it is intuitively clear and offers physical insight into the physics of the wall effects. Summarizing, he models the wing and its wake with a surface of discontinuity, uses the method of images to satisfy the wall boundary condition, assumes simple harmonic motion, and introduces the approximation

$$1/\sinh x \sim 1/x - x/6$$

His result is an approximate solution to the lift interference effect which is accurate to order λ^2 (where $\lambda = \pi b/2H$). In Ref 21, it is shown that his results may be expressed as

$$\bar{L}_R = \bar{\bar{L}}\left[1 - \frac{\lambda^2}{12}\left(\frac{-k^2 + 2ikC_R}{k^2}\right)\right] + \bar{\bar{L}}^{**}$$

$$\bar{M}_{Ra} = \bar{\bar{M}}_a + \frac{\lambda^2}{12}\left[\frac{ak^2 - (1+2a)ikC_R}{k^2}\right] b\bar{\bar{L}} - \bar{\bar{M}}_a^{**}$$

Here $\bar{L}_R$ and $\bar{M}_{Ra}$ are the total corrected aerodynamic lift and moment at or about the elastic axis. $\bar{\bar{L}}$ and $\bar{\bar{M}}$ contain all the first-order correction terms. $\bar{L}^{**}$, $\bar{M}_a^{**}$, and the expressions in brackets contain the second-order correction terms. Specifically,

$$\bar{\bar{L}} = \pi\rho b^2 [(i\omega)^2 h + U(i\omega)\alpha - ba(i\omega)^2\alpha] + 2\pi\rho UbC_T(k) \times [(i\omega)h + U\alpha + b((1/2) - a)(i\omega)\alpha]$$

$$\bar{\bar{M}}_a = \pi\rho b^2 [ba(i\omega)^2 h - b^2((1/8) + a^2)(i\omega)^2\alpha - Ub((1/2) - a)(i\omega)\alpha] + 2\pi\rho Ub^2(a + (1/2)) \times C_T(k)[(i\omega)h + U\alpha + b((1/2) - a)(i\omega)\alpha]$$

$$\bar{L}^{**} = +2\pi\rho Ub\left[\frac{iD_T}{k}\right]\frac{\lambda^2}{6}\{(i\omega)h + U\alpha + b((1/2) - a)(i\omega)\alpha\}$$

$$\bar{M}_a^{**} = 2\pi\rho Ub^2(a + (1/2))\left[\frac{iD_T}{k}\frac{\lambda^2}{6}\right]\{(i\omega)h + U\alpha + b((1/2) - a)(i\omega)\alpha\}$$

where

$$D_T = \frac{-J_0(k) + (1 - C_R)[J_0(k) - iJ_1(k)]}{\frac{\pi}{2}k\left\{Y_1(k) + f\left(\frac{k}{\lambda}\right)J_1(k) + i\left[Y_0(k) + f\left(\frac{k}{\lambda}\right)J_0(k)\right]\right\}}$$

and

$$f\left(\frac{k}{\lambda}\right) = i + \frac{2}{\pi}\int_0^\infty e^{-i(k/\lambda)}\left(\frac{1}{x} - \frac{1}{\sinh x}\right)dx$$

Note that the expressions for L and M_a are identical to those in free flight [Eq. (4)] with the Theodorsen function replaced by

$$C_R = \frac{Y_1(k) + f\left(\frac{k}{\lambda}\right)J_1(k)}{Y_1(k) + f\left(\frac{k}{\lambda}\right)J_1(k) + i\left[Y_0(k) + f\left(\frac{k}{\lambda}\right)J_0(k)\right]}$$

Timman's approach to the lift interference effect is less intuitive than Reissner's; however, it is exact. He uses velocity potential functions and conformal transformations in a manner analogous to Theodorsen's treatment of an airfoil in free flight.[11] He first transforms the problem to one which he can solve for the disturbance-velocity potential function. He then solves for the pressure distribution over the airfoil using the Bernoulli equation. Finally, by integrating the pressure distribution, he solves for the aerodynamic lift and moment. For simple flapping motion and pure rotation about midchord for a zero chamber airfoil, his results are[21]

1) Lift due to pure plunge:

$$k_a = \frac{L/\ell}{\pi\rho U^2 b} = ik\frac{16Hq^{1/2}}{\pi b}\left[T + \frac{1-T}{2}\frac{\pi^2 q^{1/2}}{K^2 k^*}s_1\right]s_1 - k^2\frac{64H^2 q}{\pi^2 b^2}s_2 \tag{6}$$

2) Moment about midchord due to pure plunge:

$$m_a = \frac{M/\ell}{\pi\rho U^2 b^2} = -ik\frac{64H^2}{\pi^2 b^2}\left[T + \frac{1-T}{2}\frac{\pi^2 q^{1/2}}{K^2 k^*}s_1\right]s_3 \tag{7}$$

3) Lift due to pure rotation about midchord:

$$k_b = k_b^{(I)} - \frac{ik_a}{k}$$

where

$$k_b^{(I)} = \frac{L^{(I)}/\ell}{\pi\rho U^2 b} = -ik\frac{16H^2 q^{1/2}\pi}{K^3 b^2 k^*}\frac{2K}{\pi}(1-T)s_1 s_3 + ik\frac{64H^2 q}{\pi^2 b^2}s_2 \tag{8}$$

4) Moment due to rotation about midchord:

$$m_b = m_b^{(I)} - \frac{im_a}{k}$$

where

$$m_b^{(I)} = \frac{M^{(I)}/\ell}{\pi\rho U^2 b^2} = ik\frac{64H^3}{K^3 b^3 k^*}\frac{2K}{\pi}(1-T)s_3^2 - k^2\frac{512H^4}{\pi^4 b^4}s_6 \tag{9}$$

In the above

$$s_1 = \sum_{m=0}^{\infty} q^m \frac{1 + q^{2m+1}}{(1 - q^{2m+1})^2}$$

$$s_2 = \sum_{n=0}^{\infty} \frac{q^{2n}}{2n+1}\frac{1 + q^{2n+1}}{(1 - q^{2n+1})^3}$$

$$s_3 = \sum_{n=1}^{\infty} \frac{1 + q^{2n}}{1 - q^{2n}}\gamma_n q^n$$

$$s_6 = \sum_{n=1}^{\infty} \frac{\gamma_n^2 q^{2n}}{n}\frac{1 + q^{2n}}{1 - q^{2n}}$$

and T is a modified Kussner T function (related to the Theodorsen function) which is given in terms of hypergeometric functions as

$$T = T(\lambda^*, k^*) = \frac{H_1 - H_0}{H_1 + H_0} = \left\{i\lambda^* F_3 - \frac{1}{\beta^{*2}}\frac{[i\lambda^* + (1/2)]}{(i\lambda^* + 1)}F_2 + \frac{1}{\beta^*}\left[\frac{2E}{Kk'^2} - 1 - i\lambda^*\frac{4k^*}{k'^2}\right]F_1\right\} \Big/ \left\{i\lambda^* F_3 - \frac{1}{\beta^{*2}}\frac{[i\lambda^* + (1/2)]}{(i\lambda^* + 1)}F_2 + \frac{1}{\beta^*}\left[\frac{2E}{Kk'^2} - 1 + i\lambda^*\frac{4k^*}{k'^2}\right]F_1\right\}$$

where

$$\lambda^* = \omega H/\pi U \quad \beta^* = e^{\pi b/H} \quad k^* = \tanh \pi b/2H \quad k' = \sqrt{1-k^{*2}}$$

and

$$F_1 = F(\tfrac{1}{2}, i\lambda^* + \tfrac{1}{2}; i\lambda^* + 1; 1/\beta^{*2})$$

$$F_2 = F(\tfrac{1}{2}, i\lambda^* + 3/2; i\lambda^* + 2; 1/\beta^{*2})$$

$$F_3 = F(\tfrac{1}{2}, i\lambda^* - \tfrac{1}{2}; i\lambda^*; 1/\beta^{*2})$$

A Common Form

Timman and Reissner both present lift and moment expressions for an oscillating, thin airfoil in a rectangular wind tunnel. Their expressions are in very different forms, however, and neither form corresponds to the equations for free flight. Having all of the results in a common form would not only allow easy comparison, but would also permit the magnitude and direction of the wall effects to be seen clearly. Timman's and Reissner's results may be written in the form

$$L = a_1 \pi \rho b^2 [(i\omega)^2 h + U(i\omega)\alpha - ba(i\omega)^2 \alpha] + a_2 2\pi \rho U b Q(k,\lambda)[(i\omega)h + U\alpha + b(a_3 - a)(i\omega)\alpha] \quad (10a)$$

$$M = a_1 \pi \rho b^2 [ba(i\omega)^2 h - b^2(a_4 + a^2)(i\omega)^2 \alpha - Ub(a_5 - a)(i\omega)\alpha] + a_2^2 \pi \rho U b^2 (a + a_5) Q(k,\lambda) \times [(i\omega)h + U\alpha + b(a_3 - a)(i\omega)\alpha] \quad (10b)$$

These are identical to the unconstrained flow equations [Eqs. (2)] except for the terms a_i and the replacement of the Theodorsen function by $Q(k,\lambda)$.

Reissner's approximate solution may be expressed in the form of Eq. (10) by expanding the expressions, dropping terms of order greater than $(\pi b/2H)^2$, and then regrouping terms.

Timman presents separate results for plunge motion and rotation about the elastic axis. Since a rotation about the elastic axis may be decomposed into a rotation about the midchord and a plunge displacement, and since the lift and moment at the elastic axis may be found if the lift and moment at the midchord are known

$$L = \pi \rho U^2 k_a\{h\} + \pi \rho U^2 b k_b\{\alpha\} + \pi \rho U^2 k_a\{-ab\alpha\} \quad (11a)$$

$$M = -\pi \rho U^2 b^2 [m_b - a m_a - a k_b + a^2 k_a]\{\alpha\} - \pi \rho U^2 b [m_a - a k_a]\{h\} \quad (11b)$$

The notation $k_a\{h\}$ indicates application of Timman's k_a operator to h. The operators k_a, k_b, m_a, and m_b are defined in Eqs. (6-9). Timman's results may be put in the form of Eq. (10) by expanding Eq. (11), identifying common factors, and then regrouping terms.

The results are presented in Tables 3-5 and Figs. 3 and 4. Table 3 defines the parameters a_i, Table 4 compares the a_i for various H/b, and Table 5 shows the dependence of Timman's a_3 on k (for each H/b). Figures 3 and 4 present comparisons of $Q_T(k,\lambda)$ and $Q_R(k,\lambda)$. (The Theodorsen function $C(k)$ is included for comparison.)

The data show roughly a 10% increase in aerodynamic lift and moment due to wall effects at $H/b = 2.0$. The data also indicate that Reissner's a_i are accurate within 2% for $H/b \geq 2$, and that on the scale of Fig. 4, $Q_R(k,\lambda)$ and $Q_T(k,\lambda)$ are indistinguishable. The error for $H/b = 1.0$ is shown in Fig. 4. Note that some of this error may be due to an inadequacy of the employed 10-point Simpson's rule integration for very small H/b. The conclusions drawn are unaffected, however.

Table 3 Definition of coefficients, a_i

$$\bar{C} = [T(s,\lambda) + 1]/2 \qquad \beta = \frac{\pi^2 q^{1/2} s_1}{K^2 k^*} \qquad \gamma = \frac{4Hq^{1/2} s_2}{\pi b s_1}$$

$$\xi = \frac{\pi^2 s_3 H}{K^3 b k^*} \qquad \lambda = \pi b/2H$$

Term	Exact (Timman)	Approximate (Reissner)	Free flight
a_1	$\frac{64H^2 q s_2}{\pi^2 b^2}$	$1+\lambda^2/12$	1
a_2	$\frac{8Hq^{1/2} s_1}{\pi b}$	$1+\lambda^2/6$	1
$a_3(s,\lambda)$	$\frac{\bar{C}(2\xi) + (\gamma - 2\xi)}{\bar{C}(2-\beta) + (\beta - 1)}$	$\frac{1/2}{1+\lambda^2/12}$	1/2
a_4	$\frac{8H^2 s_6}{\pi^2 b^2 q s_2}$	$1/8/(1+\lambda^2/12)$	1/8
a_5	$\frac{4Hs_3}{\pi b q^{1/2} s_1}$	$1/2/(1+\lambda^2/12)$	1/2
$Q(s,\lambda)$	$(2-\beta)\bar{C} + (\beta - 1)$	$C_T\left[1 + \frac{\lambda^2}{6ik}\frac{C_T^2 - D_T}{C_T}\right]$	C

Table 4 Comparison of exact (Timman) and approximate (Reissner) a_i at various H/b

H/b		10	2	1	0.5
β		1.000	1.0000	1.0000	1.0000
λ		0.4990	0.4788	0.4438	0.4004
ξ		0.2478	0.2067	0.1429	0.0767
a_1	Exact	1.0021	1.0488	1.1725	1.5191
	Approx	1.0021	1.0514	1.2056	1.8225
a_2	Exact	1.0041	1.0952	1.3209	1.8971
	Approx	1.0041	1.1028	1.4112	2.6449
$a_3(0)$	Exact	0.4990	0.4788	0.4438	0.4004
	Approx	0.4990	0.4756	0.4147	0.2744
a_4	Exact	0.1246	0.1168	0.1023	0.0827
	Approx	0.1247	0.1189	0.1037	0.0686
a_5	Exact	0.4987	0.4735	0.4299	0.3751
	Approx	0.4990	0.4756	0.4147	0.2744

One advantage to Reissner's approximate solution is that the a_i depend only on λ, making it easy to see the size and direction of the wall effects.

Examination of Fig. 3 indicates an interesting possibility. For $H/b \leq 2$, all values of $Q(k,\lambda)$ lie very nearly on the same semicircle. This suggests that $Q(s,\lambda)$ be approximated (for small H/b) as

$$Q(s,\lambda) \approx 0.5 \frac{(s/p+2)}{(s/p+1)}$$

where p is a function of H/b. This is discussed below.

Generalization to Arbitrary Motion

The aerodynamic lift and moment expressions of Eqs. (2) and (10) are written as functions of the reduced frequency k. This indicates they are valid for simple harmonic motion. To be of use to the control engineer, these equations must be extended to cover general motions of an airfoil. The central issue is the validity and form of the Theodorsen function and its equivalent $Q(k,\lambda)$.

Table 5 Dependence of Timman's $a_3(k,\lambda)$ on k and H/b

k \ H/b	$a_3(k,\lambda)$ 10	2	1	0.5
0	0.4990 +0i	0.4788 +0i	0.4438 +0i	0.4004 +0i
0.1	0.4994 +0.0008i	0.4810 0.0116i	0.4470 +0.2229i	0.4040 +0.0297i
0.15	0.4996 0.0011i	0.4835 0.0167i	0.4509 0.0326i	0.4084 +0.0438i
0.2	0.4999 0.0012i	0.4867 0.0210i	0.4559 0.0420i	0.4143 +0.0569i
0.3	0.5003 0.0013i	0.4941 0.0273i	0.4687 0.0575i	0.4296 +0.0798i
0.4	0.5006 0.0013i	0.5017 0.0307i	0.4832 0.0683i	0.4479 +0.0974i
0.5	0.5009 0.0013i	0.5085 0.0319i	0.4978 0.0749i	0.4674 +0.1098i
0.6	0.5011 0.0013i	0.5143 0.0318i	0.5114 0.0781i	0.4866 +0.1177i
0.8	0.5014 0.0012i	0.5228 0.0298i	0.5339 0.0782i	0.5209 +0.1235i
1.0	0.5016 0.0011i	0.5283 0.0271i	0.5503 0.0739i	0.5482 +0.1211i

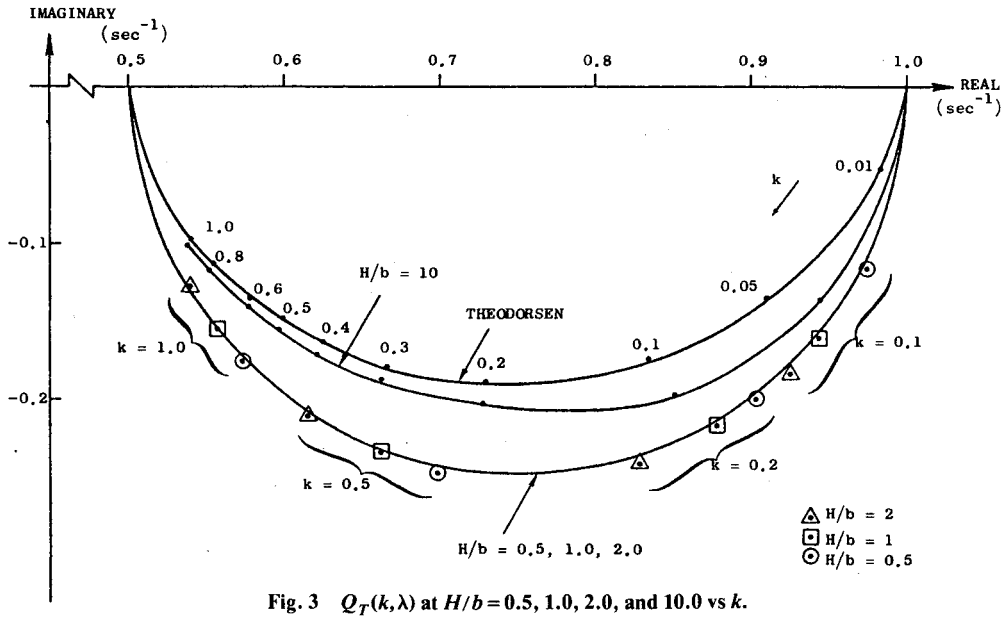

Fig. 3 $Q_T(k,\lambda)$ at $H/b = 0.5, 1.0, 2.0$, and 10.0 vs k.

Early attempts to extend the Theodorsen function into the left half of the s plane[22,23] were met with opposition.[24-27] It was not until Edwards[12] identified a derivation of the generalized Theodorsen function in the work of von Kármán and Sears[13,14] that the validity of the theory for general motion was accepted. The form of the Theodorsen function he identified is

$$C(\bar{s}) = \frac{K_1(\bar{s})}{K_0(\bar{s}) + K_1(\bar{s})}$$

This is the generalized Theodorsen function. It is identical to the familiar Theodorsen function with ik replaced by the normalized Laplace variable $\bar{s}$ ($\bar{s}=sb/U$). This function is nonrational. It is analytic everywhere except for a branch cut extending from the origin to infinity along the negative real axis. In Ref. 11, a "residue density" function is presented which describes this branch cut.

In Ref. 21, $Q_T(k,\lambda)$ is generalized by the same technique of replacing k with s. The negative real axis again becomes a critical area as it was for the generalized Theodorsen function. Here, however, there exists a distribution of poles and zeros along the axis instead of a branch cut.

The locations of the singularities of $Q_T(s,\lambda)$ are found by examining the characteristics of the hypergeometric functions F_i which comprise $T(s^*,\lambda)$. The resulting pole-zero distribution of $Q_T(s^*,\lambda)$ is depicted in Fig. 5. With the exception of the first pole and zero, all the poles and zeros

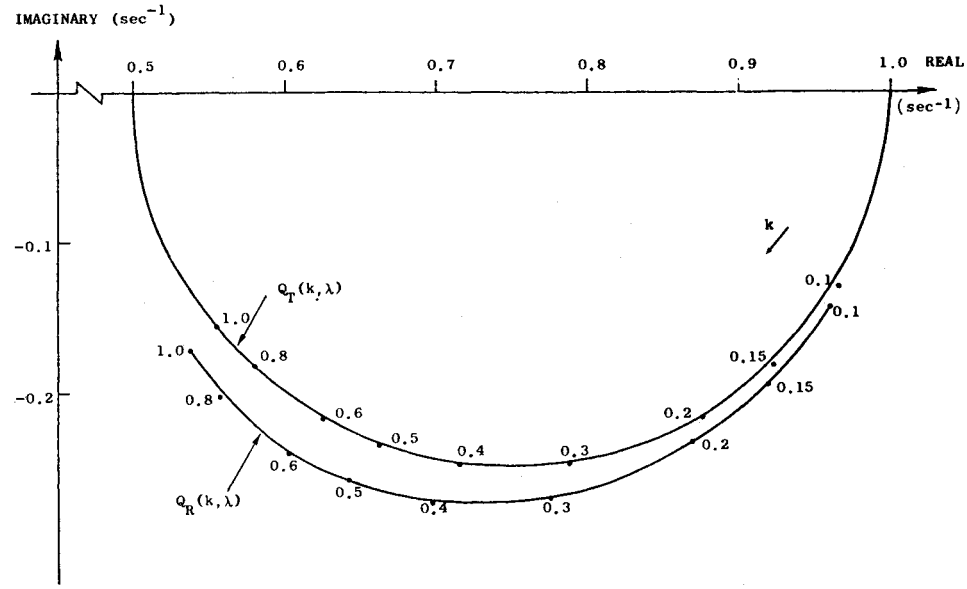

Fig.4 Comparison of $Q_T(k,\lambda)$ and $Q_R(k,\lambda)$ at $H/b=1.0$ ($\lambda=\pi b/2H$).

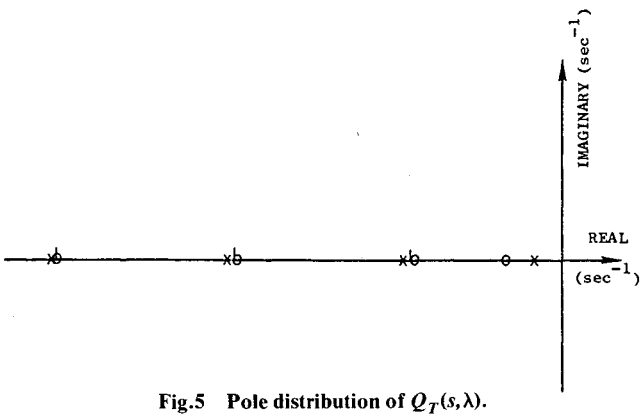

Fig.5 Pole distribution of $Q_T(s,\lambda)$.

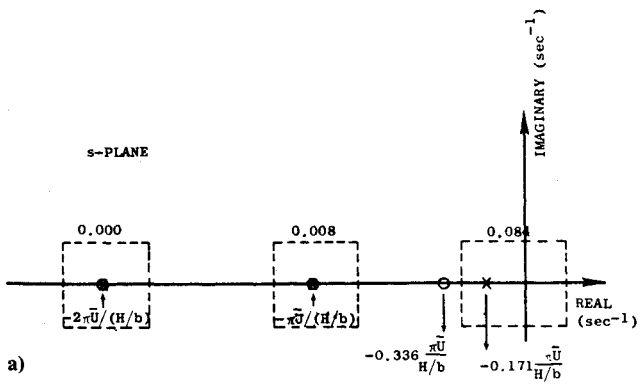

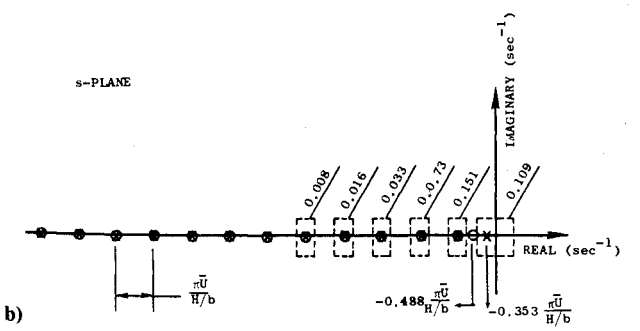

Fig. 6 a) Residues of $Q_T(s,\lambda)$ for $H/b=2$; b) residues of $Q_T(s,\lambda)$ for $H/b=10$.

appear in pairs spaced at intervals of unity in the s^*plane [$-\pi U/(H/b)$ in the s plane]. As the walls move to infinity, the spacing in the s plane approaches zero. In the limit, therefore, one has a "smear" of pole-zero pairs. This approaches a residue density of the branch cut of the $C(s)$ function.

The poles of $Q_T(s,\lambda)$ are difficult to calculate analytically. The smallest is relatively easy to find numerically, however. It occurs in the region $-U/(H/b)<s<0$ and can be located accurately using a simple numerical search since the hypergeometric functions F_i which comprise $Q_T(s,\lambda)$ are well behaved in this region. The exact locations of the remaining poles are more difficult to find, however. They occur near the points $s=-nU/(H/b)$ $(n=1,2,\ldots)$. These are singular points of the F_i, and the series used to evaluate the F_i is not accurate near these points. Consequently, a numerical search yields only approximate locations of these poles. The slight inaccuracy incurred has no effect, however, on the conclusions which will be drawn below.

Rather than locate the zeros of $Q_T(s,\lambda)$, it is easier and more useful to evaluate the residue at each of the poles. This is accomplished numerically by integrating around closed contours. Each contour encloses one pole, and the paths of integration are far enough away from the singular points of the hypergeometric functions to be in regions where the series representation is accurate. Note that this technique does not require exact knowledge of the pole locations for accurate evaluation of the residues. Figure 6 presents the results for the two cases of $H/b=2$ and 10. [The residues shown are normalized by $\pi\bar{U}/(H/b)$.] It is difficult to present results for $H/b\gg 10$ since the circles of convergence for the series representations of the F_i are approached as H/b gets large.

It is interesting to compare these discrete residue distributions of $Q_T(s,\lambda)$ with the "residue density" function which describes the branch cut of $C(\bar{s})$. Edwards[12] evaluates the "residue density" function and calls it $\mathcal{J}$. It is reproduced in Fig. 7 along with the discrete distributions calculated above. As expected, the discrete distribution tends toward the continuous function as H/b gets large.

Finite-Order Approximation

To generate a finite-order description of the equations of motion for the ideal two-DOF typical section in unconstrained flow [Eqs. (1) and (2)], approximation to the nonrational Theodorsen function is required. One widely used approximation is due to R. T. Jones[28]

$$C(s)=\frac{0.5\bar{s}^2+0.2808\bar{s}+0.01365}{\bar{s}^2+0.3455\bar{s}+0.01365} \tag{12}$$

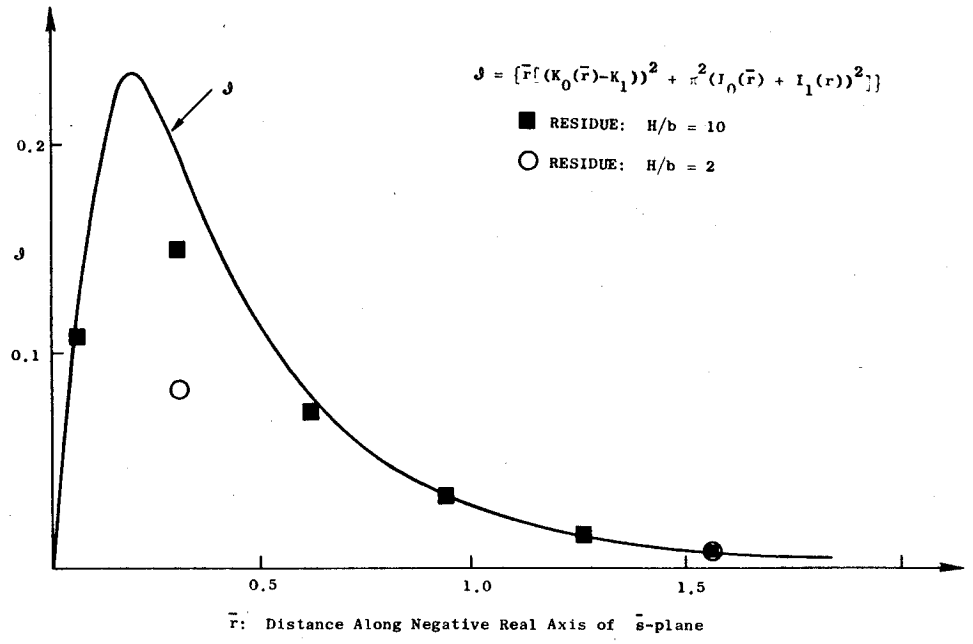

Fig. 7 Comparison of residues of $Q_T(s,\lambda)$ with Edward's residue density function, $\mathcal{J}$.

It represents a second-order fit to the magnitude and phase of $C(k)$, i.e., simple harmonic motion. Consequently, its accuracy is reliable only near the $j\omega$ axis. Edwards[12] has evaluated this function at points far removed from the $j\omega$ axis and the results indicate significant error. His results are reproduced in Fig. 8.

The equations of motion for the ideal two-DOF typical section with wind-tunnel walls present [Eqs. (1) and (10)] can also be approximated to finite order. Here, the modified Theodorsen function $Q_T(s,\lambda)$ is already rational but it contains an infinite number of poles and zeros. An approximation of arbitrary accuracy can be obtained, however, by retaining a finite number of poles and zeros. Furthermore, this approximation will be accurate throughout the entire s plane and not just near the $j\omega$ axis.

The data presented in Fig. 7 indicate that as *H/b decreases* fewer poles need to be retained to describe $Q_T(s,\lambda)$ accurately. At $H/b=2$, the residue of the first pole represents roughly 98% of the function's impulse response. Consequently, the approximation

$$Q_T(\bar{s},\lambda) \sim 0.5\frac{\bar{s}+0.538}{\bar{s}+0.269} \tag{13}$$

should describe $\bar{Q}_T(s,\lambda)$ accurately throughout the entire s plane. The data presented in Figs. 9 and 10 verify this. Figure 9 compares the single-pole approximation with the exact $Q_T(\bar{s},\lambda)$ for pure oscillatory motion (along the $j\omega$ axis), while Fig. 10 is a comparison along rays extending into the left half of the s plane. Note that in Eq. (13), the zero location was chosen to preserve the dc and high-frequency gains (1.0 and 0.5, respectively). This results in only a 2% error in the residue at $\bar{s}=-0.269$.

Experimental Verification

An airfoil and suspension has been constructed to verify experimentally the predictions of the theory discussed above. Accuracy of the theory in predicting transient motion of an airfoil in a wind tunnel was investigated.

The experimental apparatus consisted of a small (0.5 m^2), low-subsonic wind tunnel with a unique airfoil suspension design that closely approximates the ideal two-DOF typical section. The airfoil was a foam core of fiberglass-laminate with a single spar and circular endplates. It had a NACA 0009 profile with a 235 mm chord and a 413 mm span. The circular endplates were one wing chord in diameter and were installed

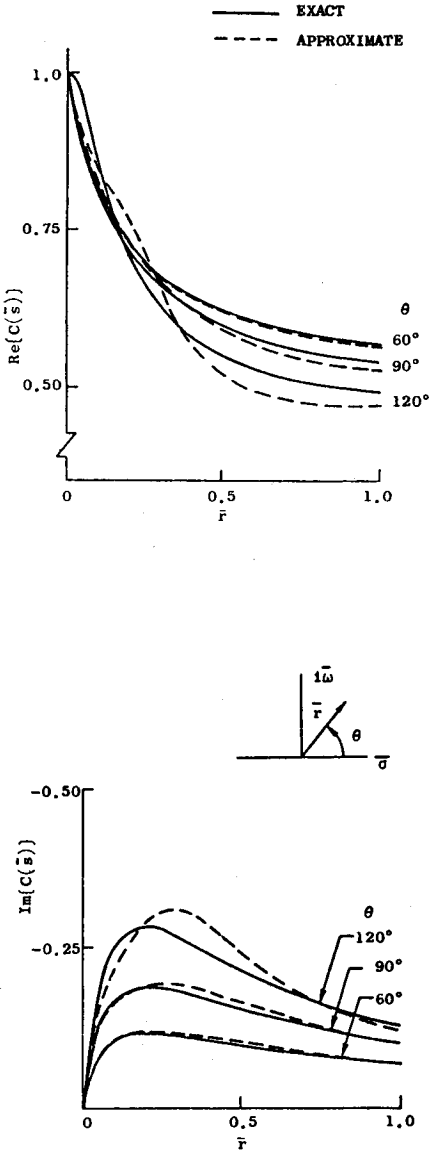

Fig. 8 Comparison of the generalized Theodorsen function and Jones second-order approximation of $C(\bar{s})$ as a function of $\bar{r}$ and θ.

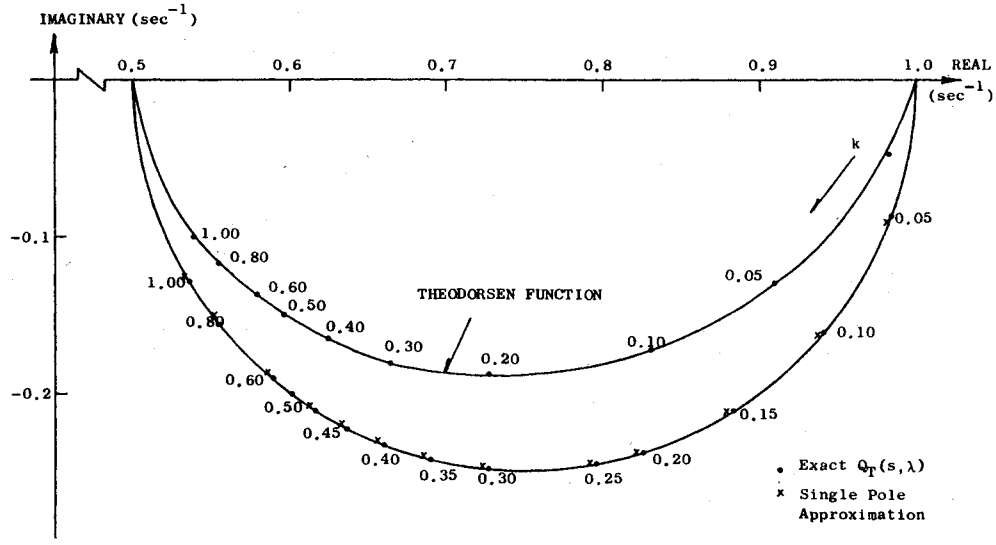

Fig. 9 Comparison of exact $Q_T(\bar{s},\lambda)$ and the single-pole approximation to $Q_T(\bar{s},\lambda)$ at $H/b=2$

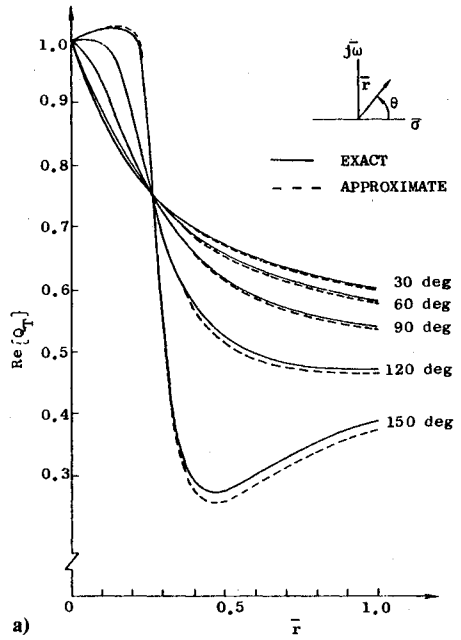

a)

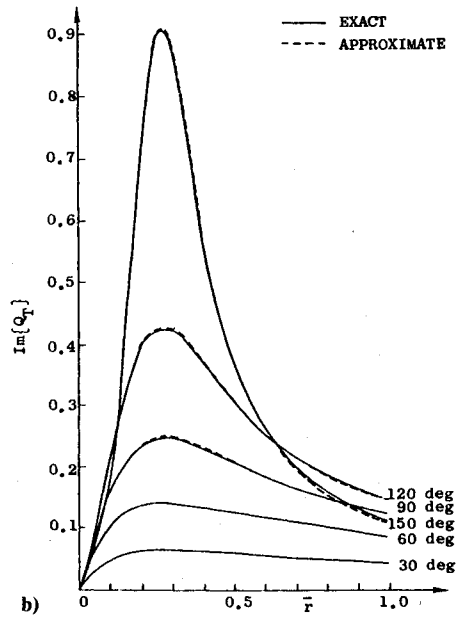

b)

Fig. 10 Comparison of $Q_T(\bar{s},\lambda)$ a) and single-pole approximation of $Q_T(\bar{s},\lambda)$; b) as a function of $\bar{r}$ and θ.

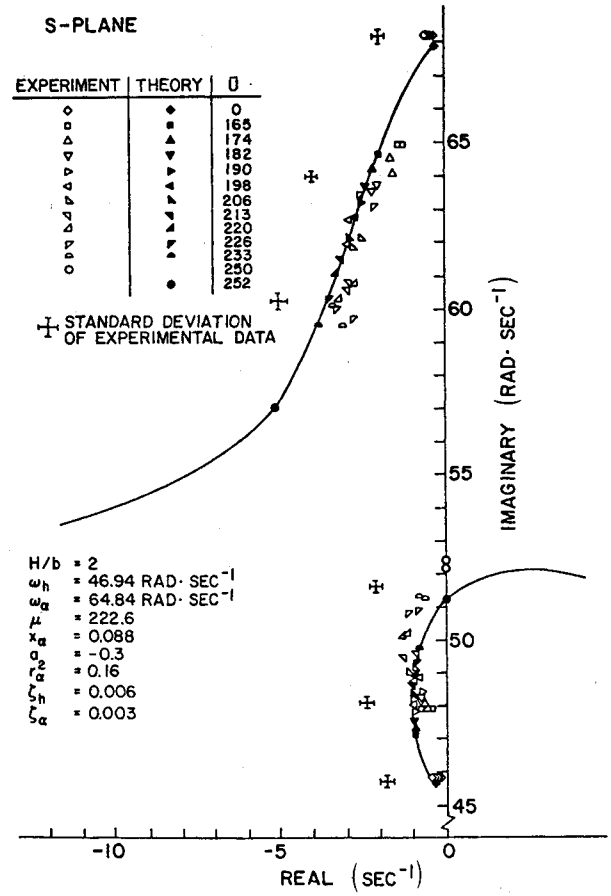

Fig. 11 Comparison of theoretical and experimental flutter loci.

to maintain two-dimensional flow over the airfoil. One endplate was attached to each end of the airfoil, and both moved with the airfoil. The endplates were located 10 mm from the tunnel walls to avoid boundary-layer effects. For this apparatus, $H/b=2$.

The suspension system constrained the airfoil to move without friction in two degrees of freedom: plunge and pitch. It provided adjustable spring rates in each degree of freedom and did not couple the degrees of freedom. The plunge suspension consisted of four metal-folded cantilevers connected by a set of machined aluminum beams. The pitch suspension consisted of torsional springs mounted in housings at each end of the wing span. All of the suspension system was external to the tunnel. Position sensors (LVDT and resolver) were provided to measure motion in each degree of freedom.

Two actuators were used, one for each degree of freedom. They could be used independently or together to simulate the effect of an aerodynamic control surface. The plunge actuator was a linear motor of the type found in computer disk drives. The pitch actuator was a brushless torque motor mounted to one end of the wing span. More detail describing the apparatus is presented in Ref. 21.

The goal of the experiment was to produce a flutter locus which could be compared with theoretical predictions. Specifically, the system's eigenvalues were determined as a function of airspeed. Data were generated by exciting the apparatus with a doublet force at various airspeeds. Data were recorded using a portable digital data acquisition system. The eigenvalues were determined by a nonlinear iterative parameter identification routine which fit the parameters of a mathematical model to match the experimental response by minimizing a quadratic output error.

Results are presented in Fig. 11. In general, the experimental data agree with the theoretical curves. The largest difference appears in the lower branch of the locus where there appears to be a systematic error which leads to a measured flutter point at a slightly lower speed than that predicted by the theory. This discrepancy is small. The flutter point predicted is $\bar{U}_f = 252\ s^{-1}$ and $\omega_f = 51.2\ s^{-1}$ while that measured in the wind tunnel is $\bar{U}_f = 250\ s^{-1}$ and $\omega_f = 52.4\ s^{-1}$. This is approximately a 1% error in the speed and a 2% error in the frequency.

The trend in the lower branch of the locus is real. It is not a systematic error produced by the analysis technique. The trend was verified by comparing the analysis results with measurements obtained from strip chart recordings.

The shift in the locus, even though it is small, is difficult to explain. The standard deviation of the experimental data is much smaller than the discrepancy, and the inaccuracies in measuring the system parameters are also incapable of explanation. A possible source of the error is non-two-dimensional flow effects. A need for a model representing some additional physical phenomenon is indicated.

Conclusions

The results presented in this paper confirm the accuracy of unsteady aerodynamic theory in predicting loadings for transient motions of an airfoil—experimentally determined eigenvalues are within 2% of their theoretical values. These results are significant since they are believed to be the first involving nonsinusoidal airfoil motion.

The scope of this study was limited to a large wing in a small subsonic wind tunnel and two-dimensional flow. Care is required when extending these results to aircraft in flight since the tunnel wall was shown to affect significantly the aerodynamic lift and moment; a 10% increase (for $H/b = 2$) is seen in the static values of lift and moment. In addition, the branch cut of the Theodorsen function is replaced by a distribution of poles and zeros.

The results of this work are specifically useful for future investigations (such as flutter suppression studies) which involve experimentation in small wind tunnels. The expressions for aerodynamic lift and moment have been developed in a convenient form which is identical to the form used in free flight, and a procedure has been presented to formulate a finite-state representation of the equations of motion which is accurate for arbitrary airfoil motion. For $H/b = 2$, a single pole-zero pair describes the modified Theodorsen function within 2% throughout the s plane, and hence, a single augmented state was adequate in the formulation of the equations of motion for the experimental apparatus.

Acknowledgment

This work was supported by the NASA Dryden Flight Research Center under Grant NSG 4002.

References

[1] Burris, P. M. and Bender, M. A., "Aircraft Load Alleviation and Mode Stabilization," AFFDL-TR-68-163, Nov. 1969.

[2] "B-52 CCV Control System Synthesis," AFFDL-TR-74-92, Vol. II, 1975.

[3] Grosser, W. F., Hollenbeck, W. W., and Eckholdt, D. C., "The C-5A Active Lift Distribution Control System," *Impact of Active Control Technology on Airplane Design,* AGARD CP-157, June 1975.

[4] Glauert, H., "Wind-Tunnel Interference on Wings, Bodies, and Airscrews," British A. R. C., R&M 1566, Sept. 13, 1933.

[5] Silverstein, A. and Joyner, U. J., "Experimental Verification of the Theory of Oscillating Airfoils," NACA TR 673, 1939.

[6] Theodorsen, T. and Garrick, I. E., "Mechanism of Flutter, a Theoretical and Experimental Investigation of the Flutter Problem," NACA Rept. 685, 1940.

[7] Reid, E. G., "Experiments of the Lift of Airfoils in Nonuniform Motion," Dept. of Aeronautics and Astronautics, Stanford University, Stanford, Calif., July 1942.

[8] "Measurements of the Aerodynamic Hinge Moments of an Oscillating Flap and Tab," USAF TR 5784, April 1949.

[9] Halfman, R. L., "Experimental Aerodynamic Derivatives of a Sinusoidally Oscillating Airfoil Two-Dimensional Flow," NACA Rept. 1108, 1952.

[10] Runyan, H. L., Woolston, D. S., and Rainey, A. G., "Theoretical and Experimental Investigation of the Effect of Tunnel Walls on the Forces on an Oscillating Airfoil in Two-Dimensional Subsonic Compressible Flow," NACA TN 3416, June 1955.

[11] Theodorsen, T., "General Theory of Aerodynamic Instability and the Mechanism of Flutter," NACA Rept. 496, 1935.

[12] Edwards, J. W., "Unsteady Aerodynamic Modeling and Active Aeroelastic Control," Ph.D. Dissertation, Dept. of Aeronautics and Astronautics, Stanford University, Stanford, Calif., SUDAAR 504, Feb. 1977.

[13] von Kármán, T. and Sears, W. R., "Airfoil Theory for Non-Uniform Motion," *Journal of Aeronautical Sciences,* Vol. 5, Aug. 1938, pp. 379-390.

[14] Sears, W. R., "Operational Methods in the Theory of Airfoils in Non-Uniform Motion," *Journal of the Franklin Institute,* Vol. 230, No. 1, July 1940, pp. 95-111.

[15] Theodorsen, T. and Garrick, I. E., "Nonstationary Flow About a Wing-Aileron-Tab Combination Including Aerodynamic Balance," NACA Rept. 736, 1942.

[16] Bisplinghoff, R. L., Ashley, H., and Halfman, R. L., *Aeroelasticity,* Addison-Wesley, Mass., 1955.

[17] Garner, H. C., Rogers, E. W. E., Acum, W. E. A., and Maskel, E. C., "Subsonic Wind-Tunnel Wall Corrections," AGARDograph 109, Oct. 1966.

[18] Pope, A. and Harper, J., *Low Speed Wind Tunnel Testing,* John Wiley & Sons, New York, 1966.

[19] Reissner, E., "Wind Tunnel Corrections for the Two-Dimensional Theory of Oscillating Airfoils," Cornell Aeronautical Laboratory, Ithaca, N. Y., Rept. SB-318-S-3, 1947.

[20] Timman, R., "The Aerodynamic Forces on an Oscillating Aerofoil Between Two Parallel Walls," *Applied Science Research* (The Hague), Vol. A3, No. 1, 1951, pp. 31-57.

[21] Rock, S. M., "Transient Motion of an Airfoil: An Experimental Investigation in a Small, Subsonic Wind Tunnel," SUDAAR 513, Dept. of Aeronautics and Astronautics, Stanford University, Stanford, Calif., SUDAAR 513, May 1978.

[22] Jones, W. P., "Aerodynamic Forces on Wings in Non-Uniform Motion," British A. R. C., R&M No. 2117, Aug. 1945.

[23] Luke, Y. and Dengler, M. A., "Tables of the Theodorsen Circulation Function for Generalized Motion," *Journal of Aeronautical Sciences,* Vol. 18, July 1951, pp. 478-483.

[24] Van de Vooren, A. I., "Generalization of the Theodorsen Function to Stable Oscillations," *Journal of Aeronautical Sciences,* Vol. 19, March 1952, pp. 209-211.

[25] Laitone, E. V., "Theodorsen's Circulation Function for Generalized Motion," *Journal of Aeronautical Sciences,* Vol. 19, March 1952, pp. 211-213.

[26] Jones, W. P., "The Generalized Theodorsen Function," *Journal of Aeronautical Sciences,* Vol. 19, March 1952, p. 213.

[27] Chang, C., "On Theodorsen Function in Incompressible Flow and C-Function in Supersonic Flow," *Journal of Aeronautical Sciences,* Vol. 19, Oct. 1952, pp. 717-718.

[28] Jones, R. T., "The Unsteady Lift of a Wing of Finite Aspect Ratio," NACA Rept. 681, 1940.